THERMAL EFFECT OF PHASE TRANSFORMATIONS IN HIGH SILICON CAST IRON

Marcin STAWARZ, Krzysztof JANERKA, Jan JEZIERSKI, Jan SZAJNAR

Silesian University of Technology, Faculty of Mechanical Engineering, Department of Foundry Engineering Gliwice, Poland, EU, marcin.stawarz@polsl.pl

Abstract

The results of the experiments on the high-silicon cast iron crystallization have been presented in the paper. The researches have been focused on the transformations in solid state during the crystallization process. The temperature changes have been recorded during the experiments. The temperature first derivative as a time function has been calculated what made possible to estimate some characteristic points (fields) of the crystallization process. Thanks to these results the phase transformations description has been elaborated. Two foundry alloys with Si content below and above 15% have been used for the melts. Additionally, the attempt of the influence of the heat transfer rate from the mould on the alloy morphology estimation has been made. The inspiration for such approach was to describe the factors influencing the crystallization process e.g. chemical analysis, casting parameters, mould cooling conditions etc. and their influence on the alloy overall quality. The target were especially intermetallic phases i.e. Fe_5Si_3 characteristic for alloys with higher Si concentration. There is a lack of scientific literature in this topic and a lot of them is quite obsolete and what is more some data are mutually contradictory. The data according to the alloy matrix microstructure is ambiguous when the upper limit of 15%Si is exceeded. Some sources claim 100% of silicon ferrite while the other claim some percentage of iron silicide. The crystallization process parameters influence on these phases growth has not been described in the literature, yet.

Keywords: silicon cast iron, crystallization, intermetallic phases, thermal derivative analysis, quality control

1. INTRODUCTION

The high-silicon cast iron it is an iron-carbon alloy containing 12 ÷ 18% Si and manganese, phosphorus and sulphur. Though the alloy contains approx. 1%C it is called cast iron because its solidification occurs in the eutectic temperature range [1,2,3]. ASTM standard [4] defines three high-silicon iron grades, divided regarding to carbon, chromium and molybdenum concentration. Si content in all grades (Grade 1, Grade 2, Grade 3) is the same an equals 14.20-14.75% Si. The high-silicon cast iron is corrosion resistant material. Its resistance increases with silicon content increase, however, the minimum Si content which gives it corrosion resistance is around 14% [5]. Acid resistance of high-silicon cast iron depends on the SiO_2 thin layer created on the casting surface. The Fe atoms are flushed out the surface and the remained atoms combine with the oxygen and the protective layer is created. The oxidizing environment makes the protective properties of the layer higher and after the mechanical damage the layer can regenerate itself due to oxidisers activity [2]. With alkalis the silicon dioxide creates soluble silicates (Na_2SiO_3, K_2SiO_3), while with the hydro fluoride creates silicon tetra fluoride SiF_4 in gaseous form. The creation of such compounds results in high-silicon iron lack of resistance in contact with the compounds containing these chemicals [2]. This iron is resistant for inorganic acids oxidizing (nitric, sulphuric, chromic etc.) and their solutions with organic acids in wide range of concentration and temperature. In some cases (e.g. with HNO_3) this resistance is high up to the boiling point [2].

The high-silicon iron possess not only good acid resistance but it is wear resistant, too, so this alloy is often used in manufacturing of pumps for slime transportation [5]. Often, when silicon content is less than 12.5% the alloy possess better fluidity and mechanical properties, especially ductility but the corrosion resistance significantly decreases [6]. This feature is going down with the carbon content increase and graphite precipitations growth. The next disadvantageous phenomenon is segregation especially of silicon. It results in

non-uniform passive layer thickness and causes its different increment in time. These conditions promote electrochemical corrosion [6]. The harmful contaminations in high-silicon cast iron are calcium and aluminium, which create non-metallic inclusions what causes bigger porosity and less acid resistance as well as worsen casting properties of the material [2]. The alloy has a tendency to create intermetallic phases (due to increased Si content). This intermetallic phases are mostly of Fe_5Si_3 type (i.e. iron silicate). The literature data about this subject is quite poor and sometimes ambiguous. What is connected to the crystallization process of such an iron and the conditions for these phases appearance there is no data at all or it is only vestigial.

2. EXPERIMENTAL PART

2.1 The experimental stand

The research method was based on high-silicon cast iron laboratory melts series and the alloy crystallization parameters recording for several thermal conditions. The main research tool during the examinations was Thermal Derivative Analysis (DTA), which is based on temperature changes recording and its time derivatives analysis. The experimental stand view was shown in **Fig. 1**.

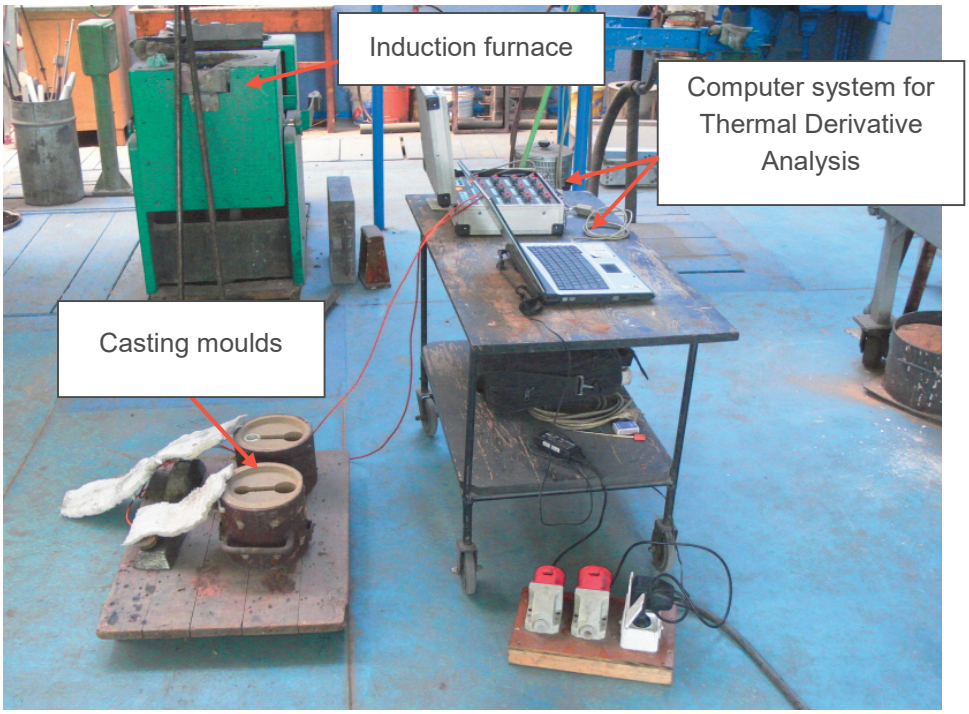

Fig. 1 The experimental stand for the temperature in time changes recording

2.2 The experimental conditions

The cast iron melt was carried out in 50kW induction furnace of frequency 60 Hz [7]. The charging materials were melted down, the carburizer was introduced [8] and then the metal bath was overheated up to 1400 °C. The next step was liquid alloy cooling (slowly, along with furnace cooling) down to 1200 °C. This operation's goal was to remove all gases dissolved in molten metal. Then the liquid metal bath was heated up to1350 °C. Liquid alloy was poured into hot foundry ladle and then poured into moulds (samplers) for the temperature changes recording (thermal derivative analysis DTA). Two different heat transfer rates were achieved thanks to mould cavity construction modification [9]. The Sibral® insert use resulted in thermal conductivity decrease down to λ=0.342 W/(m·K) [9]. The second mould (sampler) was made on quartz sand base and bentonite, so this moulding sand thermal conductivity is inside the range of 0.4 W/(m·K) in

100ºC ÷ 0.7 W/(m·K) in 1000ºC [9]. The Si content in the alloy being examined was over 15% in first and under 15% Si in the second case. During both experiments the influence of the heat dissipation rate from the mould on final cast iron microstructure was analysed. The temperature changes with cooling time were observed and first temperature derivative was calculated, too.

2.3 Test results

Figs. 2 - 5 show the recorded temperature changes in time for different rates of heat transfer and various silicon content in alloy. The first derivative was calculated. The calculations results in graphical form in figures 2 - 5 were shown. Thermal effects in the solid state are visible on the graph, too. Thermal effect as a result of transition in solid state was marked with vertical discontinuous line on the figures. Transition temperature corresponds to the thermal effect of phase transformation from Fe_2Si to Fe_5Si_3 [10÷11]. Maximum thermal effect of phase transitions was observed in 991 ºC (*case a*) and 990 ºC (*case b*). In the figures 4 and 5 (cast iron with Si content below 15 %) the recorded temperature changes (along with the temperature first derivative) were presented. The thermal effect from the Fe_2Si phase transition into Fe_5Si_3 was not observed.

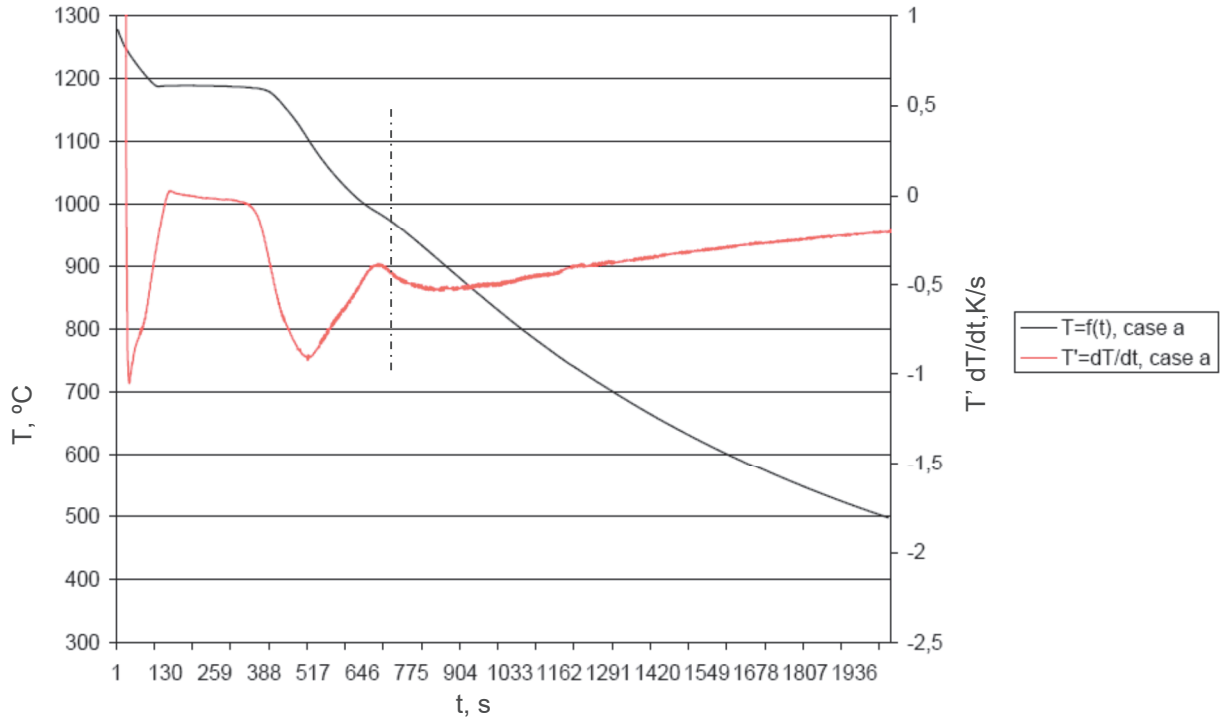

Fig. 2 TDA curves for casting moulds with aluminosilicate fibres plug (*case 'a'*), silicon content over 15 %

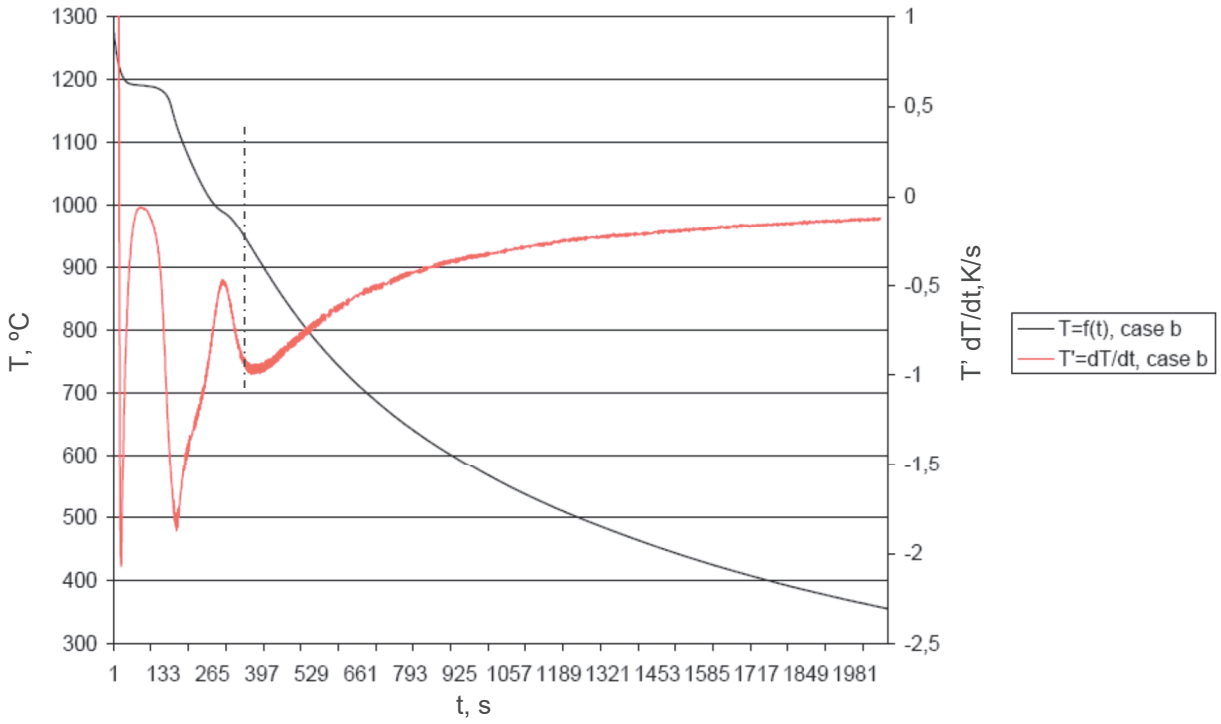

Fig. 3 TDA curves for casting moulds without aluminosilicate fibres plug (*case 'b'*) silicon content over 15 %

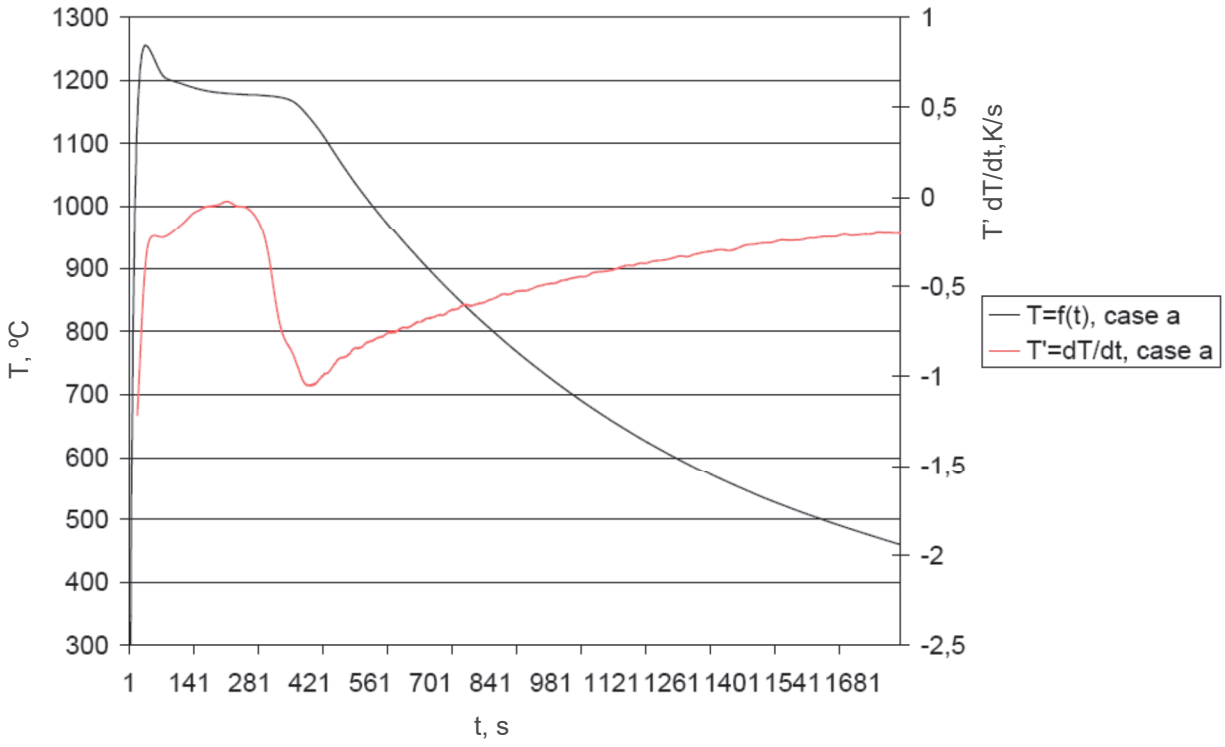

Fig. 4 TDA curves for casting moulds with aluminosilicate fibres plug (*case 'a'*), silicon content under 15 %

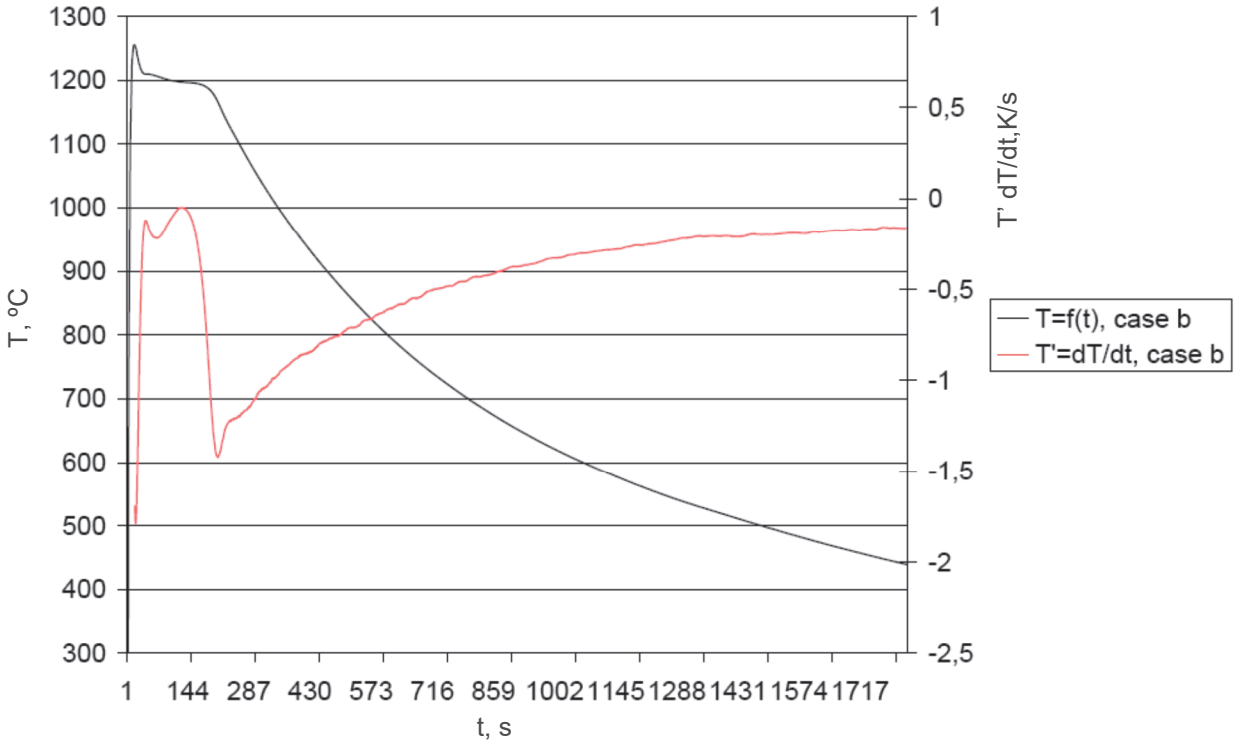

Fig. 5 TDA curves for casting moulds without aluminosilicate fibres plug (*case 'b'*), silicon content under 15 %

Below in the **Fig. 6** the microstructure photographs of the produced cast iron with Si content over 15% were shown. Base on microstructure metallographic analysis the graphite precipitations were observed (black features on the photographs), the metal matrix components: silicon-ferrite (bright area) and intermetallic phase Fe_5Si_3 precipitations (black fields).

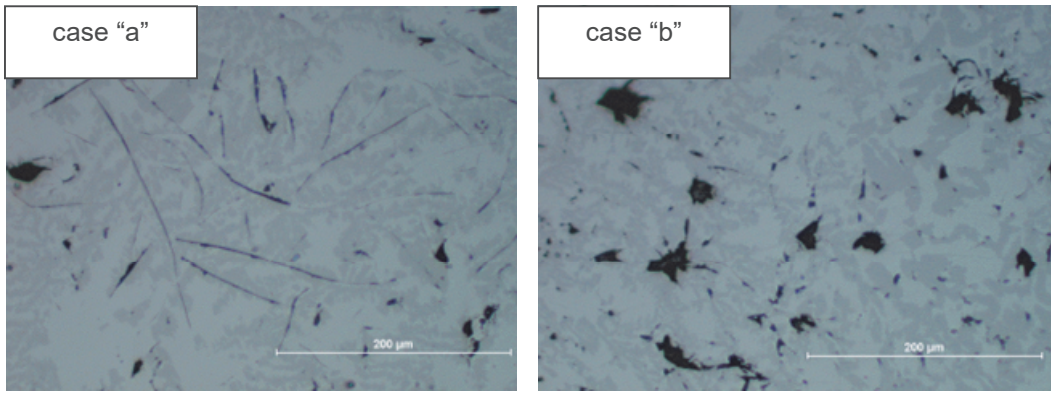

Fig. 6 Microstructure for casting moulds with aluminosilicate fibres plug (*case a*) and without (*case 'b'*), silicon content over 15 %

The metallographic analysis of the castings microstructure for the Si content under 15% shown the graphite precipitations and a metal matrix consisted of 100% silicon-ferrite (bright area on the photographs). Because these samples had a huge amount of gases absorbed (a lot of gaseous pores) the photographs were not included in the paper. It is almost impossible to recognize on the photographs whether the visible features are graphite precipitations or gaseous pores and only live microscopic examination make this distinction possible.

CONCLUSIONS

In solid state in the case of castings with Si content over 15 % three microstructure constituents were determined and these are graphite precipitations, Fe_5Si_3 phases [9÷11] and silicon-ferrite matrix. Characteristic point registered on the DTA curve (**Fig. 2** and 3 - 990°C and 991°C) corresponds with thermal effect from transition of Fe_2Si phase into Fe_5Si_3 phase. The maximum thermal effect in solid state for the transition Fe_2Si into Fe_5Si_3 in both cases is similar (though the heat transfer conditions are different for both casting moulds) and the only 1°C difference was observed. In solid state for the castings with Si content under 15% the graphite precipitations were identified together with metal matrix consisted of silicon-ferrite. The metallographic examinations proved the derivative thermal analysis (DTA) results. On the presented graphs (**Fig. 4** and 5) the characteristic thermal effects from the Fe_2Si into Fe_5Si_3 phases were not observed. The next (planned) experimental step will be stereological description of the high-silicon cast iron microstructure and an attempt to combine statistically all of the results (stereological and thermal analyses) taking into consideration casting mould thermal transfer parameters and their influence on the intermetallic phases presented in the alloy.

REFERENCES

[1] SAKWA W.: *Żeliwo*. Wyd. "Śląsk" Katowice 1974, (in Polish).

[2] PODRZUCKI C.: *Żeliwo. Struktura właściwości zastosowanie*. Tom 2. Wyd. ZG STOP. Kraków 1991. p. 295-301, (in Polish).

[3] LACAZE J., SUNDMAN B. An Assessment of the Fe-C-Si System. Metallurgical Transactions A Volume 22a, October 1991. p. 2211-2223.

[4] *ASTM A 518/A 518M - 99 Standard Specification for Corrosion-Resistant High-Silicon Iron Castings (Reapproved 2003) ASTM, 2003.*

[5] SAKWA W., Odlewy o podwyższonych własnościach, Skrypty uczelniane Nr 408, wyd. Politechnika Śląska, Gliwice, 1973, (in Polish).

[6] HENDERIECKX, G.D. *Silicon Cast Iron*. Gietech BV, 2009

[7] SZAJNAR J., WALASEK A., BARON C. The zone without carbon in alloy layer obtained on steel cast. Manufacturing Technology Vol. 13, No. 1/2013, p 103-108.

[8] JANERKA K., JEZIERSKI J., SZAJNAR J. The evaluation of effectiveness of liquid cast iron recarburization process by using different carburizers and methods of recarburization. 20th Anniversary International Conference on Metallurgy and Materials METAL, 18. - 20. 5. 2011, Brno, Czech Republic.

[9] STAWARZ M. Influence of technological parameters on the microstructure of the silicon cast iron, 22nd International Conference on Metallurgy and Materials, Metal 2013, May 15-17.2013, Brno, Czech Republic, p. 92-96.

[10] STAWARZ M. Aspekty wytwarzania żeliwa wysokokrzemowego w warunkach przemysłowych. Archives of Foundry Engineering, Vol. 11, Special Issue 3/2011, p. 205 - 208, (in Polish).

[11] STAWARZ M. Żeliwo wysokokrzemowe, zapomniany materiał odporny na korozję - problemy podstawowe. Ochrona przed korozją, vol. 55, nr 5, 2012, p 235.